Surface modification of zeolite and kaolin with 3-(aminopropyl) triethoxysilane and 3-(trimethoxysilyl) propyl methacrylate

C. Özel[1], C. Akat[1], R. Alosmanov [2], M. U. Kahveci[3], C. Emir[1], S. Yücel[1*]

[1]Yildiz Technical University, Faculty of Chemical and Metallurgical Engineering, Department of Bioengineering, Istanbul, Turkey
[2] Bakü State University Faculty of Chemistry, Department of High-Molecular Compounds Chemistry, Bakü, Azarbeijan
[3]İstanbul Technical University, Chemistry Department, İstanbul, Turkey

Zeolites are crystalline, hydrated aluminosilicates of alkaline earth cations composed of 3-dimensional frameworks, which have been widely used for adsorbents, catalysts, ion exchangers, molecular sieves for separation, and sorting the molecules according to their crystalline size dimensions. Kaolin is an industrial clay, consisting of hydrated aluminum silicate mineral, named kaolinite. Kaolin is used for various purposes in paper coating and filling, ceramics, cracking catalysts, and many other uses. Kaolin functions as pharmaceutical excipient in commercial products, such as granulating agent, film-coating additive, anti-caking agent and also accelerates blood clotting. Surface modification of kaolin allows it to be used in different industries and for different purposes. Surface modification of inorganic materials can be carried out by means of silanol agents. (3-Aminopropyl) triethoxysilane (APTES), 3-(trimethoxysilyl) propyl methacrylate (MPTMS), (3-aminopropyl) trimethoxysilane (APTMS) are known important silanization agents used for surface modification. The aim of this study is the surface modification of a zeolite and kaolin with APTES and MPTMS at different ratios and in different solvent media (ethanol, toluene, DMSO). The structures of the samples were investigated using zeta potential, Fourier transform infrared analysis (FTIR) and scanning electron microscopy (SEM). It was determined that the optimum APTES modification ratio for zeolite was 1:10 in toluene, while the optimum MPTMS modification ratio of kaolin was 1:3. It was revealed that the layered structure of kaolin is interleaved with DMSO solvent.

Keywords: Zeolite, Kaolin, APTES, MPTMS, Silanization.

INTRODUCTION

Zeolite structures consist of SiO_4 and AlO_4 primary units. About 100 different architectures are known which are based on vertex-sharing SiO_4 and AlO_4 tetrahedra and these units are into a truncated octahedron. Zeolites are used in several areas such as laundry detergents, oil refining and petrochemical industries, adsorbents, gas separations, agriculture and major application areas as adsorbents, catalysts, and ion exchange material. Although not as good as silica gel and aluminum oxide, zeolites also have high water adsorption capacity [1–3]. However, the adsorption capacity decreases depending on the temperature increase. Zeolite is used in biomedical applications due to its antibacterial and biocompatibility properties. Surface modified zeolites provide advantageous and beneficial usage in various specific biomedical application areas such as drug delivery, soft and hard tissue applications, hemostatic agents. For example, products containing zeolite applied directly to the wound are used by the United States (US) military to stop bleeding and create hemostasis. Rapid and on-site blood loss can be intervened by using zeolite and zeolite-containing products in frequently occurring traffic accidents, domestic injuries, and war wounds. It functions as a practical and easy-to-use absorbent material that dehydrates the blood and adheres to the injured tissue and provides hemostasis to prevent deaths due to blood loss [4–6]. Zeolite can be used as an absorbent material that can dehydrate blood, adhere to injured tissue, and induce hemostasis [7].

Kaolin occurs in a layered structure and is composed of sheets of Si tetrahedral and Al octahedral with common oxygen, with the formation of a 1:1 layer [8]. It has two different basal cleavage faces [9]. One basal face consists of a tetrahedral siloxane surface with very inert Si-O-Si links. The other basal surface consists of an octahedral, gibbsite $(Al(OH)_3)$ sheet [10]. Kaolin is an important mineral in the world market. Kaolin can be used as an additive that can improve the properties of materials by modifying the surface. These materials are used in paper coating and filler, ceramics, paint, plastic, rubber, fiberglass, cracking catalysts and many other uses. Functions as a pharmaceutical excipient in commercial products; It is a granulating agent, film coating additive, diluent, pelletizing agent, suspending and anti-caking agent, it also

accelerates blood coagulation [11]. Kaolin has also been observed to accelerate the cessation of bleeding by activating the hemostatic factors Factor XII, Factor X, Factor V, and platelets. More importantly, kaolin has good biocompatibility.

In order to improve the good mechanical property and biocompatibility to the biomedical implants consisting of surface modification of substrates has been widely studied in the past years. Surface modification by APTES containing a high density of primary amino groups was reported to be a reliable way to bind a protective film with good biocompatibility [12]. Owing to the protonation of amino groups, bioactive matters, or drug carrier systems could be immobilized on the surface through zwitterionic pairs. Two different surface modifications of kaolin and zeolite can occur. The physical modification takes place by affecting the chemical composition and by the use of high temperatures. Chemical modification occurs by changing the structure, surface functional groups and surface area by organic compounds, acids or bases [13]. (3-Aminopropyl) triethoxysilane (APTES), 3-(trimethoxysilyl) propyl methacrylate (MPTMS), (3-aminopropyl) trimethoxysilane (APTMS) are known important silanization (silane-coupling) agents used for surface modification of materials. Silanization is a low-cost and very effective covalent coating method for modifying the surface of materials containing large numbers of hydroxyl groups. Bonding of silicon-based molecules on zeolite or kaolin occurs when hydroxyl groups on surfaces can bind to silicon atoms. There are many types of commercially available silanization agents. They are easy to react with a hydroxylated surface and introduce active groups (e.g., amino group and carboxyl group) to the surface of the material [14]. The aim of this study is to perform surface modifications of zeolite and kaolin using different ratios of APTES and MPTMS, as well as in different solvents (ethanol, toluene, DMSO). The characterization of the samples was peerformed by zeta potential analysis, FTIR and SEM analysis.

EXPERIMENTAL

Inorganic substrates used in this study, zeolite and kaolin, surface modification agents APTES and MPTMS, silanization agents, solvents ethanol (EtOH), toluene (T) and dimethyl sulfoxide (DMSO) were commercially obtained from Merck (KGaA, Darmstadt, Germany).

Surface modification studies of the zeolite were carried out by using different ratios (1:4, 1:5, 1:10, 1:40, 1:80 (w/v) in toluene, 1:4 in ethanol) of the silanization agent APTES. All samples are presented in Table 1. In order to obtain a zeolite-APTES 1:5 (w/v) ratio, initial 0.05 g amount of zeolite was weighed and dried in a moisture analyzer RADWAG MA 50.R (Bracka, Poland) at 105 °C. Then the zeolite was dispersed in 5 mL of toluene for 15 min in an ultrasonic water bath. Then, 250 µl of APTES was added dropwise to the mixture at 100 °C for 24 hours. To eliminate unbound silanization agents, it was centrifuged at 9000 rpm for 10 min, and washed 3 times. The amine-modified zeolite obtained after washing was dried using a vacuum oven at 50 °C. Other zeolite-APTES ratios were prepared by applying the same method.

The kaolin substrate surfaces were treated with different ratios of MPTMS silanization agent (1:3, 1:5, 1:10 (w/v) with/without DMSO). 1 g of kaolin was weighed and dried in a moisture analyzer at 105 °C. Kaolin was dispersed in 9 mL of DMSO and 1 mL of water at 60 °C for 10 days. DMSO expands the layers of kaolin (intercalation effect) and activates the more active -SH groups instead of -OH groups [15]. Then, this solution was brought to room temperature, the mixture was centrifuged at 9000 rpm for 10 min, and the washing process with toluene was repeated 5 times. It was dried in a vacuum oven at 50 °C. Dried kaolin (1 g) was treated with 5 mL of MPTMS at 150 °C for 2 days, in order to obtain a kaolin-MPTMS ratio of 1:5. Then, this solution was brought to room temperature, the mixture was centrifuged at 9000 rpm for 10 min, and the washing process with toluene was repeated 5 times. It was dried in a vacuum oven at 50 °C. To see the effect of DMSO, the same procedures were done without using DMSO. Other kaolin-MPTMS ratios were prepared by applying the same method.

Table 1. Ratios and abbreviations used in zeolite and kaolin surface modification

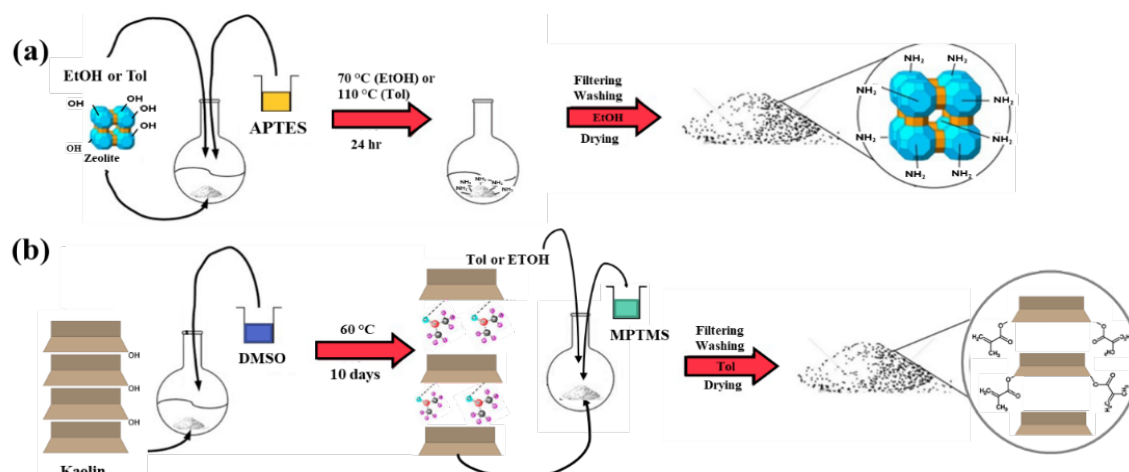| Component	Ratio	Abbreviation
Zeolite:APTES: EtOH	1:4	ZAE-4
Zeolite:APTES:T	1:4	ZAT-4
Zeolite:APTES:T	1:5	ZAT-5
Zeolite:APTES:T	1:10	ZAT-10
Zeolite:APTES:T	1:40	ZAT-40
Zeolite:APTES:T	1:80	ZAT-80
Kaolin:DMSO		KD
Kaolin:MPTMS: EtOH	1:5	KME-5
Kaolin:MPTMS:T	1:5	KMT-5
Kaolin:DMSO: MPTMS	1:3	KDM-3
Kaolin:DMSO: MPTMS	1:5	KDM-5
Kaolin:DMSO: MPTMS	1:10	KDM-10

Figure 1. Scheme of modification of (a) zeolite with APTES and (b) kaolin with MTMS. The zeta potential measurement after the surface modification with MPTMS after DMSO intercalation showed that it increased up to -4.39 mV, but it did not increase in direct proportion to the MPTMS ratio.

Characterization

Zeta Potential Analysis

The zeta potentials (ζ potential) distribution for zeolite and kaolin by Zetasizer Nano ZS (Malvern Instruments, Worcestershire, UK) instrument with 4.0-mV He–Ne laser (633 nm) at 25 °C and scattering angle of 90° were measured. Samples suspensions were homogenized using an ultrasonic probe. Zeta potential distribution was determined with the help of the laser Doppler electrophoresis method. The analysis was repeated three times. The electrophoretic mobility of the particles is automatically calculated and converted into the zeta potential. The zeta potential measurements were performed in phosphate buffer solution (PBS).

Fourier Transform Infrared Spectrometric (FTIR) Analysis

FTIR spectroscopy was used to understand the effect of physicochemical methods on the surface chemistry of modified zeolite and kaolin. FTIR spectra were collected and recorded in the region of 650-4000 cm^{-1} on a FTIR spectrophotometer (IR Prestige-21, Shimadzu, Japan). Prior to analysis, modified zeolite and kaolin samples were placed in a vacuum oven at 50 °C for 24 hours and kept in a desiccator to avoid contact with air humidity.

Scanning Electron Microscopy (SEM)

SEM analysis will examine the surface morphologies and distribution of surface-attached polymer chains in composites. Au coating was applied for all samples before scanning.

Statistical Analysis

The results are presented as mean ± SD and the degree of statistical significance was calculated by t-test, considering a significance level at $p < 0.05$.

RESULTS AND DISCUSSION

In the present study, zeolite and kaolin were modified with two different silanization agents, APTES and MPTMS, respectively, in different ratios and different solvent media for determining the optimum silanization agent ratio for further biomedicine applications. Different ratios used in surface modification were investigated successfully for surface modification of zeolite and kaolin. APTES modified zeolite and MPTMS modified kaolin were prepared following the procedure shown in Figure 1. For zeolite modifications, different ratios of APTES were prepared in toluene or ethanol and dried. On the other hand, kaolin was modified with MPTMS with or without DMSO to investigate the intercalation effect. The prepared materials were characterized by zeta potential, FTIR, and SEM analysis.

Zeta Potential Analysis

The value of the zeta potential is a sign of the surface charge and stability of a material that importantly affects the modification of the material. Besides, large values of zeta potential (above 30 mV positive values or below -30 mV negative values) indicate great electrostatic repulsive interplays between materials, meaning less agglomeration [16]. Zeta potential of APTES modified zeolites is shown in Figure 2(a). The zeta potential result of zeolite was -24.4 ± 1.22 mV. This is due to the hydroxyl (OH) groups on the surface of zeolites [17]. As a result of the modification of zeolites with APTES in ethanol and toluene, it was observed that the zeta potentials approached positive

-14.87 ± 0.47 and -7.23 ± 0.87 mV, respectively. It showed that the zeta potential results in the APTES modification with toluene had less negative value and thus more of the NH_2 group with a positive charge, which is consistent with the literature data. Therefore, it was decided to use toluene solvent for further modification. It was observed that the zeta potential of APTES modified zeolites is positive with the increase in the ratio of APTES (from -7.23 to +5.62 mV). Besides, it was observed that treatment of zeolites only in solvents without using APTES had little effect on their zeta potentials. Zeta potential value of zeolite in ethanol is -18.33 ± 0.87 and in toluene -17.53 ± 0.93 mV (data not shown).

The results of the zeta potentials of kaolin were examined, it was observed that kaolin has also a negative zeta potential due to the OH groups on the surface, such as zeolite. The zeta potential of KD appeared to be -27.2 ± 0.98 mV, which was due to the negative charges of the -SH groups of DMSO. The kaolin modifications without DMSO treatment were examined, it was observed that the zeta potentials of these samples increased negatively in the MPTMS modification in toluene and ethanol. Similarly to the zeolite sample, toluene was a more effective solvent for kaolin. The zeta potential measurement after the surface modification with MPTMS after DMSO intercalation showed that it increased up to -4.39 mV, but it was observed that it did not increase in direct proportion to the MPTMS ratio.

FTIR Analysis

Figure 3 shows the FTIR spectra of the zeolite and APTES-modified zeolites. The peaks at wavenumbers 673 and 960 cm^{-1} represent the symmetric stretching of Si–Al–O and symmetrical stretching Si-O groups present in the structure of the zeolite. The peak observed at 1655 cm^{-1} wavenumber
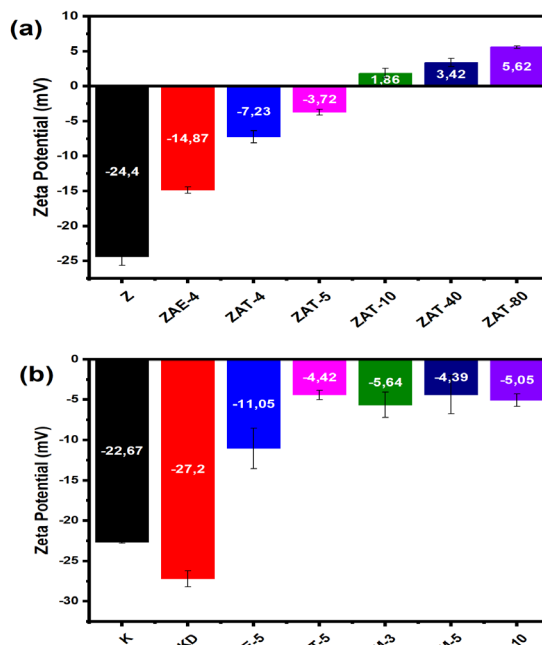

Figure 2. Zeta potential of (a) zeolite and (b) kaolin particles.

represents the –OH groups, bending vibration of physically adsorbed water molecules on zeolite surface. The wide peak at 3690-3200 cm^{-1} shows the -OH stretching vibration of the zeolite [19, 20]. Figure 3(a) represents the zeolite (Z), ZAE-4 and ZAT-4 FTIR spectra. One of the APTES, which was observed around 1644 cm^{-1}, is the peak belonging to the NH_2 group. This peak refers to "the N–H bending vibration of primary amine" in the aminopropyl group in the structure of APTES [21]. The peaks of aliphatic –CH, –CH_2, –CH_3 stretching vibrations appeared in the ZAT-5 sample at a wavenumber of 2930 cm^{-1}. The increased intensity of absorption peaks in the range of 1500–1300 cm^{-1}, representing the Si–CH_2 and Si–CH_3 stretching vibrations of silane groups, was successfully demonstrated in the
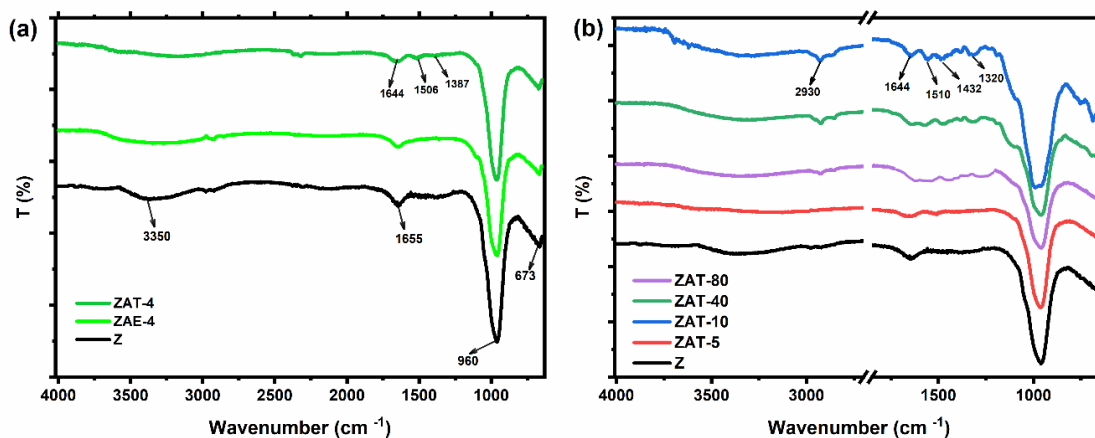

Figure 3. FTIR spectra of (a) zeolite modification in toluene and ethanol and (b) zeolite modifications at different APTES ratio.

ZAT-5 sample. This clearly shows that APTES on the surface of the zeolite binds successfully on ZAT-5 sample [22]. Therefore, it was determined to use toluene as an efficient solvent for further APTES modifications. Figure 3(b) shows the FTIR spectra of APTES zeolite samples at different ratios. It was observed that the characteristic peaks of APTES increased proportionally as the APTES ratio increased. The ZAT-10 sample is the first sample with a positive zeta potential and was chosen as the optimum ratio for APTES modification because it was the first sample to show that it was adequately modified with APTES in the FTIR spectra.

FTIR spectra of kaolin (K) and MPTMS modified kaolin are shown in Figure 4. Kaolin has Si tetrahedral and Al octahedral layers [8]. While the peaks observed at 3697, 3669 and 3653 cm^{-1} in the FTIR spectrum of kaolin indicate interlamellar hydroxyl (–OH) groups in the Al octahedral layers, the peak at 3618 cm^{-1} indicates hydroxyl groups in the intralamellar structure [15, 23]. Peaks observed at 1114, 1001, and 786 cm^{-1} wavenumbers indicate regular Si-O and Al-O bending vibrations in the kaolin structures and the poorly discrete peaks established to the Si-O stretching vibrations [24]. By intercalation of DMSO to kaolin, hydroxyl group peaks at 3697 and 3618 cm^{-1} were maintained, but the peak intensity at 3697 cm^{-1} decreased. Besides,

in Figure 4(b) new peaks were emerging in the FTIR spectrum of KD sample. Peaks at 3018 and 2936 cm^{-1} showed the stretching vibration absorption of –CH_3 groups and the peaks at 1433, 1401, 1394 and 1318 cm^{-1} were attributed to bending vibration in DMSO in the kaolin layers. All these results suggested hydrogen bond formation between the outer Al–OH of the kaolin layer and the S=O groups of DMSO molecules [23].

On the FTIR spectrum of KDM-5 sample, peaks for inter- and intralamellar hydroxyls groups were detected at 3699 cm^{-1}, and 3618 cm^{-1} while intralamellar hydroxyls peaks are not shown. The peak observed at 1720 cm^{-1} was attributed to C=O. Peaks at 2945 and 1470 cm^{-1} represent symmetric and asymmetric stretching of the CH_3 and CH_2 groups, respectively [15, 25]. All KDM samples were observed to be successfully modified with MPTMS silanization agent. However, the aforementioned peaks could not be observed in the samples modified without DMSO treatment like KTM-5 and KEM-5 (see Figure 4(a)). Similar to the zeta potential results, Figure 4(c) shows that the KDM-3, KDM-5 and KDM-10 samples have the same characteristic peak intensities. Therefore, KDM-3 was found with the optimum ratio for MPTMS modification of kaolin.
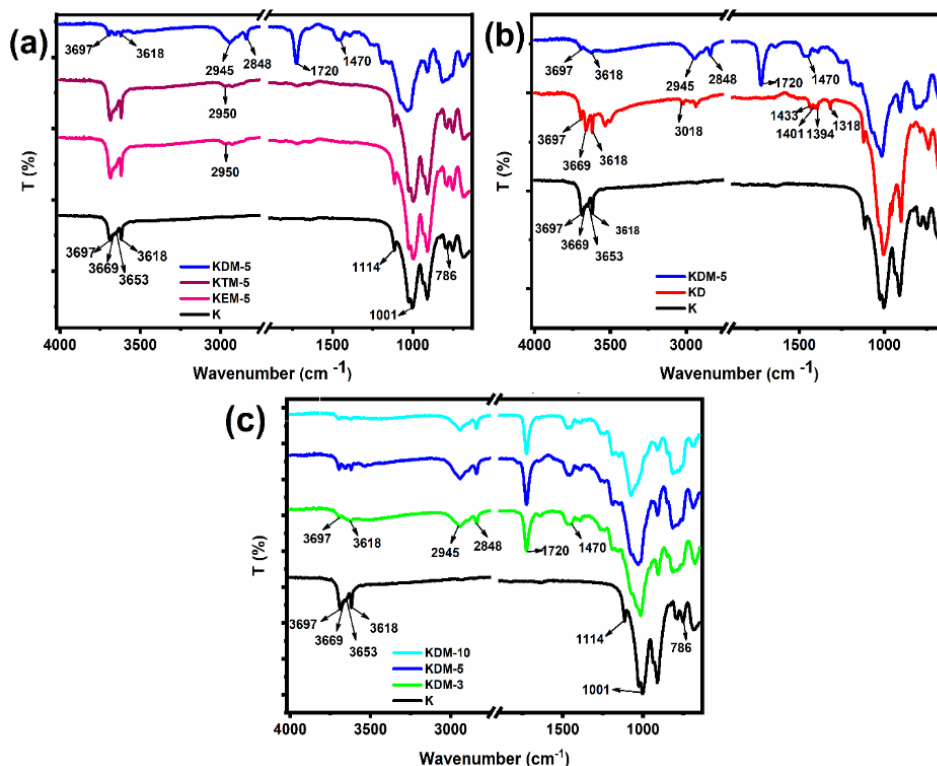

Figure 4. FTIR spectra of kaolin modification (a) in toluene, ethanol and only MPTMS (b) DMSO and MPTMS and (c) at different MPTMS ratios.

SEM Analysis

Figure 5 shows the SEM image of zeolite and ZAT-10 samples. The morphology of the zeolite was found to be irregular three-dimensional cubic structure with a diagonal length of about 4 μm. The morphology of the ZAT-10 particles was found irregular and asymmetric spherical-like shape rather than cubic shape. The zeolite surfaces were quite rough and discontinuous [26]. Aggregation was observed in both zeolite and ZAT-10. ZAT-10 tends to form larger aggregates due to new adhesive forces between the amine functional groups, compared to zeolites [27].
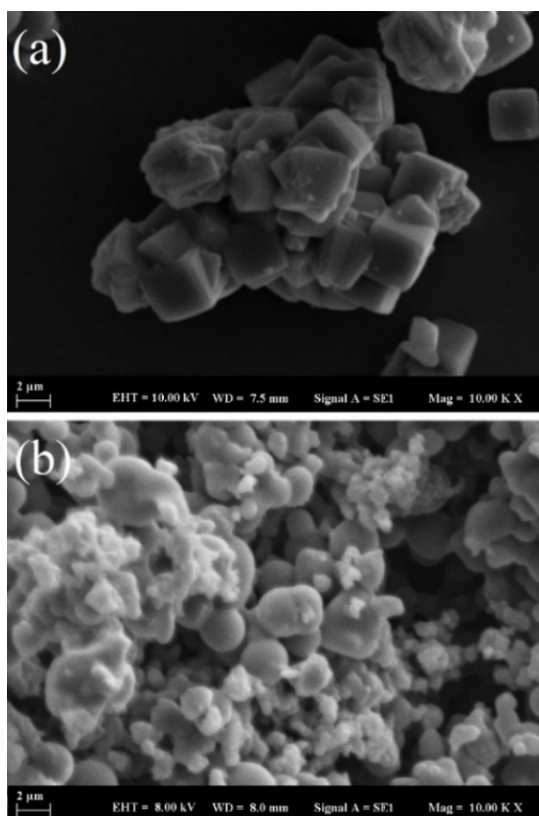

Figure 5. SEM images of (a) K and (b) KDM-5 samples

The morphology of the kaolin and KDM-5 particles was observed with SEM as illustrated in Figure 6. The structure of raw kaolin was proven to have platy, layered structure, and its morphology to be book-like in SEM images [28, 29]. After intercalation with DMSO and modification with MPTMS, adjacent layers were delaminated and distances between layers were expanded. In Figure 6(b), it is seen that the book-like kaolin is separated into layers and these particles are disordered and randomly dispersed [28]. Low zeta potential value of KDM-5 sample has allowed to adhere to particles themselves and caused aggregation.
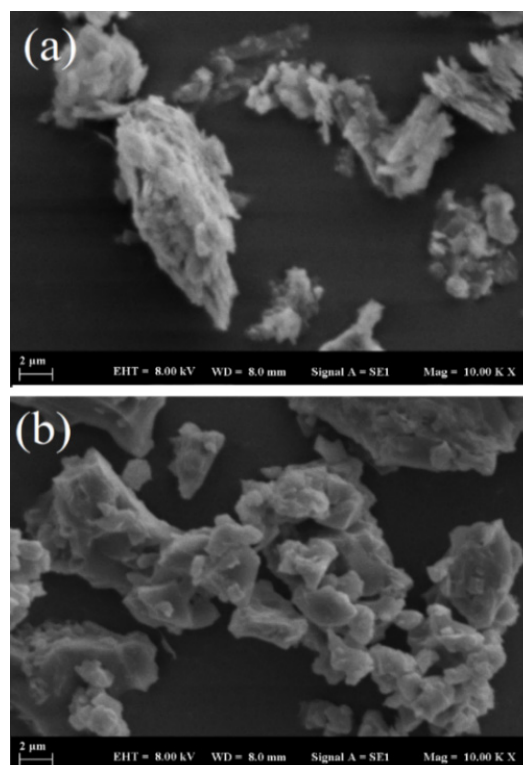

Figure 6. SEM images of (a) zeolite and (b) ZAT-10 samples

CONCLUSION

In summary, we introduced zeolite and kaolin modification with silanization agents, APTES and MPTMS, respectively. Samples were characterized using FTIR, SEM, and zeta potential analysis. In conclusion, the surfaces of zeolite and kaolin were successfully modified with silanization agents in toluene solution. Increasing concentration of APTES caused increased peak intensity, while by increasing concentration of MPTMS, intensity of peaks remained constant. The kaolin layered structures were delaminated by DMSO. The optimum ratio for modification of zeolite with APTES was found to be 1:10 (w/v), while for kaolin with MPTMS it was 1:3 (w/v).

REFERENCES

1. P. A. Jacobs, E. M. Flanigen, J. C. Jansen, H. van Bekkum, Introduction to Zeolite Science and Practice, Elsevier, Amsterdam, The Netherlands, 2001.
2. P. Terzioğlu, S. Yücel, M. Öztürk, *Water Sci. Technol.,* **75**, 358 (2017).
3. P. Terzioğlu, S. Yucel, *BioResources* **7**, 5435 (2012).

4. L. M. Jurkić, I. Cepanec, S. K. Pavelić, K. Pavelić, *Nutr. Metab. (Lond).,* **10**, 1 (2013).

5. H. B. Alam, Z. Chen, A. Jaskille, R. I. L. C. Querol, E. Koustova, R. Inocencio, R. Conran, A. Seufert, N. Ariaban, K. Toruno, P. Rhee, *J. Trauma - Inj. Infect. Crit. Care,* **56**, 974 (2004).

6. M. C. Neuffer, J. McDivitt, D. Rose, K. King, C. C. Cloonan, J. S. Vayer, *Mil. Med.,* **169**, 716 (2004).

7. J. K. Wright, J. Kalns, E. A. Wolf, F. Traweek, S. Schwarz, C. A. K. Loeffler, W. Snyder, L. D. Yantis, J. Eggers, *J. Trauma - Inj. Infect. Crit. Care,* **57**, 224 (2004).

8. M. Massaro, C. G. Colletti, G. Lazzara, S. Riela, *J. Funct. Biomater.,* **9**, 58 (2018).

9. C. S. J. Hurlbut, Dana's Manual of Mineralogy, 18th ed., John Wiley & Sons Ltd, New York, NY, USA, 1971.

10. D. J. A. Williams, K. P. Williams, *J. Colloid Interface Sci.,* **65**, 79 (1978).

11. M. E. Awad, A. López-Galindo, M. Setti, M. M. El-Rahmany, C. V. Iborra, *Int. J. Pharm.,* **533**, 34 (2017).

12. C. Wang, G. Zhang, Z. Li, Y. Xu, X. Zeng, S. Zhao, J. Deng, H. Hu, Y. Zhang, T. Ren, *Tribol. Int.,* **137**, 46 (2019).

13. D. Panda, S. K. Singh, E. Anil Kumar, in: Advances in Energy Research, Springer, Singapore, 2020, p. 541.

14. M. Aliofkhazraei, in: Handbook of Nanoparticles, Springer International Publishing, Switzerland, 2016.

15. B. F. Ferreira, K. J. Ciuffi, E. J. Nassar, M. A. Vicente, R. Trujillano, V. Rives, E. H. de Faria, *Appl. Clay Sci.,* **146**, 526 (2017).

16. I. S. Grover, S. Singh, B. Pal, *Appl. Surf. Sci.,* **280**, 366 (2013).

17. T. Kuzniatsova, Y. Kim, K. Shqau, P. K. Dutta, H. Verweij, *Microporous Mesoporous Mater.,* **1**–**3**, 102 (2007).

18. E. Tiryaki, Y. Başaran Elalmış, B. Karakuzu İkizler, S. Yücel, *J. Drug Deliv. Sci. Technol.,* **56**, 101517 (2020).

19. F. Jamshaid, M. R. Dilshad, A. Islam, R. U. Khan, A. Ahmad, M. Adrees, B. Haider, *Microporous Mesoporous Mater.,* **309**, 110579 (2020).

20. W. H. Flank, in: Molecular Sieves—II, ACS publications, 1977, p. 43.

21. I. A. Rahman, M. Jafarzadeh, C. S. Sipaut, *Ceram. Int.,* **35**, 1883 (2009).

22. L. D. Anbealagan, T. Y. S. Ng, T. L. Chew, Y. F. Yeong, S. C. Low, Y. T. Ong, C.-D. Ho, Z. A. Jawad, *Membr.,* **11**, 630 (2021).

23. H. Qu, S. He, H. Su, *Sci. Reports,* **9**, 1 (2019).

24. L. Domka, N. Stachowiak, A. Malicka, *Polish J. Chem. Technol.,* **10**, 5 (2008).

25. I. M. F. Lopes, K. Abersfelder, P. W. Oliveira, S. H. Mousavi, R. M. R. Junqueira, *J. Mater. Sci.,* **53**, 11367 (2018).

26. H. Li, J. Xu, J. Wang, J. Yang, K. Bai, J. Lu, Y. Zhang, D. Yin, *J. Membr. Sci.,* **471**, 84 (2014).

27. H. Sanaeepur, A. Kargari, B. Nasernejad, *RSC Adv.,* **4**, 63966 (2014).

28. H. Cheng, Q. Liu, J. Zhang, J. Yang, R. L. Frost, *J. Colloid Interface Sci,.* **348**, 355 (2010).

29. H. Wang, C. Li, Z. Peng, S. Zhang, *J. Therm. Anal. Calorim.,* **105**, 157 (2011).